Nano Energy 46 (2018) 29–38

Contents lists available at ScienceDirect

Nano Energy

journal homepage: www.elsevier.com/locate/nanoen

Full paper

Heterostructured nanorod array with piezophototronic and plasmonic effect for photodynamic bacteria killing and wound healing

Xin Yu[a,b,1], Shu Wang[a,c,1], Xiaodi Zhang[a,c], Anhui Qi[a], Xiran Qiao[a], Zhirong Liu[a,c], Mengqi Wu[a,c], Linlin Li[a,c,*], Zhong Lin Wang[a,c,d,*]

[a] Beijing Institute of Nanoenergy and Nanosystems, Chinese Academy of Sciences, Beijing 100083, PR China
[b] Institute for Advanced Interdisciplinary Research, University of Jinan, Jinan 250022, PR China
[c] School of Nanoscience and Technology, University of Chinese Academy of Sciences, Beijing 100049, PR China
[d] School of Materials Science and Engineering, Georgia Institute of Technology, Atlanta, GA 30332-0245, USA

ARTICLE INFO

Keywords:
Bacteria killing
Wound healing
Photodynamic therapy
Piezophototronic effect
Localized surface plasmon resonance (LSPR)

ABSTRACT

Bacteria induced infectious diseases have threated the lives and health of millions people each year. Nanosized titanium dioxide (TiO_2) have been developed for photodynamic bacterial killing with minimal drug resistance, but the efficiency was restricted by their large band gap, limited light-absorption region, and rapid electron-hole recombination. In this work, we rationally fabricated a TiO_2/BTO/Au multilayered coaxial heterostructured nanorod array by inserting a ferroelectric semiconductor barium titanate ($BaTiO_3$) nanolayer between TiO_2 nanorod and gold nanoparticles (AuNPs). The TiO_2/BTO/Au heterostructure showed greatly enhanced reactive oxygen species (ROS) (superoxide ($O_2^{\bullet-}$) and hydroxyl radicals (•OH)) generation, and incident photo-electron conversion efficiency (IPCE) in UV/visible light region. On the basis of experimental observations, the detailed photodynamic mechanism of the enhanced ROS generation was proposed, mainly ascribed to the piezophototronic effect and plasmonic property of the nanorod array. The nanorod array was used as an antibacterial coating to kill gram-negative bacterium *E. coli* and gram-positive bacterium *S. Aureus* with an antibacterial efficiency up to 99.9% under simulated sunlight. It also showed an efficient promotion of infectious wound regeneration in mice with *S. aureus* infected dermal wounds.

1. Introduction

In the past several decades, the abuse of antibiotics for conquering bacteria induced infectious diseases have triggered antibiotic-resistant bacteria, which bring serious problem to human health and eco-environment [1,2]. New alternative antibacterial agents and antibacterial methodologies without antibiotics, *e.g.* photodynamic therapy (PDT), have been developed as a minimally invasive therapeutic modality to conquer multidrug resistance bacteria. PDT takes advantage of photo-induced reactive oxygen species (ROS) generation with photosensitizers, including peroxides (H_2O_2), superoxide ($O_2^{\bullet-}$), hydroxyl radicals (•OH), and singlet oxygen ($^1O_2$) [3]. When used for antibacterial application, the ROS in intimate contact with bacteria would induce the peroxidation of the polyunsaturated phospholipid component of the lipid membrane and promote the disruption of the cell respiration to destroy bacteria [4].

Titanium dioxide (TiO_2) nanomaterials, the most widely used inorganic photocatalyst, could absorb ultraviolet (UV) light to catalyze the ROS generation [5]. Recent researches found that TiO_2 had the highest generation rate of •OH and $^1O_2$ and minimum dark toxicity to avoid harms to normal tissues, compared with inorganic metallic oxide nanoparticles (*e.g.,* ZnO, CeO_2) [6–8]. However, with wide band gap (BG) (3.0–3.2 eV) [9–11], TiO_2 can only absorb and utilize high-energy UV light, which has limited tissue penetration, and also would damage normal tissues at high dose [12]. Moreover, their antibacterial application is remarkably hindered by the limited amount of ROS generation due to the fast recombination of photoexcited electrons (e^-) and holes (h^+) pairs. To overcome these obstacles, noble metal nanoparticles with localized surface plasmon resonance (LSPR) especially gold nanoparticles (Au NPs) have been composited with TiO_2 to form Schottky barrier for the catalytic enhancement [13–15]. The metal nanoparticles can extend the light absorbance from UV to visible region with the assistance of plasmonic effect. Hot-electron injection and plasmon-induced resonance energy transfer are also considered to be main mechanisms for the plasmonic enhancement of photocatalysis [16]. As to the mechanism of hot-electro injection, it is proposed that the

* Corresponding authors at: Beijing Institute of Nanoenergy and Nanosystems, Chinese Academy of Sciences, Beijing 100083, PR China.
E-mail addresses: lilinlin@binn.cac.cn (L. Li), zhong.wang@mse.gatech.edu (Z.L. Wang).
[1] These authors contributed equally to this work.

https://doi.org/10.1016/j.nanoen.2018.01.033
Received 22 December 2017; Received in revised form 12 January 2018; Accepted 19 January 2018

photogenerated hot electrons from Au could be transferred into the conduction band (CB) of neighboring n-type semiconductor, leaving behind holes as the redox centers [17]. However, the energy band alignment of TiO_2 and Au is energetically unfavorable, which unsatisfies the direct transfer of electrons from Au to TiO_2 [18]. Therefore, promotion of the charge separation and transfer to further enhance the photochemical ROS generation is greatly desired for practical antibacterial application.

Piezoelectric and ferroelectric nanomaterials such as ferroelectric $BaTiO_3$ and $LiNbO_3$, multiferroic $BiFeO_3$, and piezoelectric semiconductor ZnO represent a special class of materials with the ability of electrical modulation. These materials have been widely used in the fabrication of photovoltaic and energy harvesting devices [19–21]. Recently, the piezoelectric and ferroelectric property has been used for the promotion of photoinduced electrons-holes separation for photocatalysis *via* building an internal piezoelectric potential [22,23]. With this performance, we hypothesized the rational design of the nanocomposites with a piezoelectric potential may have the ability to promote photodynamic bacterial killing.

In this work, a multilayered coaxial heterostructured nanorod array made with $TiO_2/BaTiO_3/Au$ is successfully synthesized to construct an internal piezoelectric field between TiO_2 and Au. The $BaTiO_3$ nanolayer is deduced to enhance the transportation of the LSPR electrons from Au into TiO_2, which depresses the recombination and promotes the photoinduced PDT. With the enhancement of photoelectrochemical performance, the nanorod array was used as a skin antibacterial coating for photodynamic bacterial killing and infectious skin wound healing *in vitro* and *in vivo*. The nanorod array as an antibacterial coating was able to kill bacterial with an antibacterial efficiency up to 99.9% under simulated sunlight.

2. Results and discussion

Fig. 1a illustrates the preparation process of the multilayered coaxial TiO_2/BTO/Au nanorod array. Firstly, TiO_2 nanorod array was epitaxially gown on a fluorine-doped tin oxide (FTO) substrate *via* a hydrothermal reaction [24]. The outermost layer of the TiO_2 nanorod was subsequently converted to $BaTiO_3$ by *in situ* reaction in the presence of barium precursor through an ion-exchange process. The thickness of $BaTiO_3$ nanolayer could be controlled by tuning the reaction time and barium precursor concentration. Au NPs were then deposited on the TiO_2/BTO core/shell nanorod *via* a physical vapor deposition (PVD) process. For inducing the ferroelectric polarization, a positive polarization (+3 V for 5 min) was exerted to the samples using Pt sheet as the counter electrode in a 2 M KCl electrolyte. The final antibacterial coating has a multilayer TiO_2/BTO/Au coaxial heterostructure on the substrate. The one-dimensional (1D) nanorod array structure with the well-defined exposed crystal facets and high surface area would facilitate the enhancement of light absorption and charge transportation [25].

Fig. 1b–d shows scanning electron microscopy (SEM) images of the top and cross-sectional view of the TiO_2/BTO/Au coaxial heterostructure. Highly aligned nanorods with tetragonal crystallographic planes (*ca.* ~ 2.5 μm in the thickness and 50–150 nm in the nanorod diameter) were observed, and small gold nanoparticles could be discerned (Fig. 1d inset). The high resolution transmission electron microscope (HRTEM) images (Fig. 1e–g) show the surface layer of the TiO_2 nanorod had been successfully converted to tetragonal $BaTiO_3$ (lattice fringe d_{111} = 0.232 nm), distinguishable from interplanar distance of d_{110} = 0.325 nm of rutile TiO_2. The TiO_2/BTO interface was fairly coherent with good lattice match. The $BaTiO_3$ shell thickness was measured to be 5–7 nm, above the critical thickness (~ 2.4 nm) for $BaTiO_3$ to show ferroelectricity at room temperature [26]. A great number of gold nanoparticles (d_{111} = 0.235 nm, face-centered cubic gold) with a mean diameter of about 5 nm were evenly decorated on the surface of the nanorods. Some of the Au NPs had close distance to each other (< 1 nm), which may induce strong local electromagnetic field enhancement *via* the LSPR effect. The multilayered coaxial heterostructure was further proven by element mapping (Fig. 1h), which showed the Au NPs were located at the outmost layer. The positive polarization of TiO_2/BTO/Au with a 3 V voltage had no observable effect on the morphology.

The X-ray diffraction (XRD) results of $TiO_2/BaTiO_3/Au$ showed the peaks from rutile TiO_2, tetragonal $BaTiO_3$ and face-centered cubic Au (Figs. 2a and S4 in the Supporting information). The diffraction peaks located at 26.5°, 33.8°, 37.9°, 51.7°, 61.7°, and 65.8° were indexed to

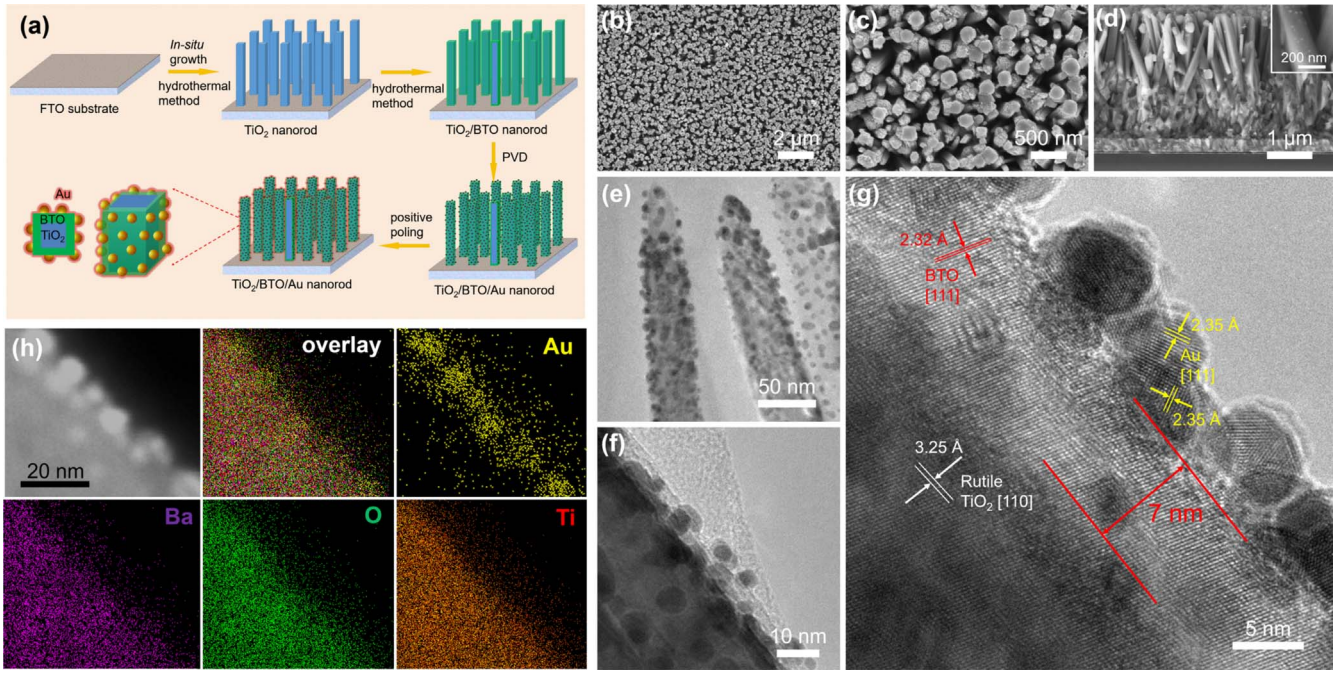

Fig. 1. Fabrication and morphology of TiO_2/BTO/Au nanorod array. (a) Scheme of fabrication process of TiO_2/BTO/Au nanorod array. (b–d) SEM images, (b, c) top surface view, and (d) cross-sectional view of TiO_2/BTO/Au nanorod, (e, f) TEM images and (g) HRTEM image of TiO_2/BTO/Au nanorod, (h) TEM image and EDX element mapping of TiO_2/BTO/Au.